THE JOURNAL OF BIOLOGICAL CHEMISTRY VOL. 288, NO. 48, pp. 34384–34393, November 29, 2013

Analysis of *Drosophila* Glucuronyl C5-Epimerase

*IMPLICATIONS FOR DEVELOPMENTAL ROLES OF HEPARAN SULFATE SULFATION COMPENSATION AND 2-O-SULFATED GLUCURONIC ACID**

Received for publication, July 3, 2013, and in revised form, September 30, 2013 Published, JBC Papers in Press, October 16, 2013, DOI 10.1074/jbc.M113.499269

Katsufumi Dejima[‡], Masahiko Takemura[‡], Eriko Nakato[‡], Jesse Peterson[‡], Yoshiki Hayashi[‡], Akiko Kinoshita-Toyoda[§], Hidenao Toyoda[§], and Hiroshi Nakato[‡1]

From the [‡]Department of Genetics, Cell Biology, and Development, University of Minnesota, Minneapolis, Minnesota 55455 and [§]Faculty of Pharmaceutical Sciences, Ritsumeikan University, Shiga 525-8577, Japan

Background: The physiological significance of C5-epimerization of glucuronic acid (GlcA) remains elusive.
Results: *Drosophila Hsepi* mutants are viable and fertile with only minor morphological defects, but they have a short lifespan.
Conclusion: Sulfation compensation and 2-*O*-sulfated GlcA contribute to the mild phenotypes of *Hsepi* mutants.
Significance: The findings suggest novel developmental roles of 2-*O*-sulfated GlcA.

During the biosynthesis of heparan sulfate (HS), glucuronyl C5-epimerase (Hsepi) catalyzes C5-epimerization of glucuronic acid (GlcA), converting it to iduronic acid (IdoA). Because HS 2-*O*-sulfotransferase (Hs2st) shows a strong substrate preference for IdoA over GlcA, C5-epimerization is required for normal HS sulfation. However, the physiological significance of C5-epimerization remains elusive. To understand the role of Hsepi in development, we isolated *Drosophila Hsepi* mutants. Homozygous mutants are viable and fertile with only minor morphological defects, including the formation of an ectopic crossvein in the wing, but they have a short lifespan. We propose that two mechanisms contribute to the mild phenotypes of *Hsepi* mutants: HS sulfation compensation and possible developmental roles of 2-*O*-sulfated GlcA (GlcA2S). HS disaccharide analysis showed that loss of *Hsepi* resulted in a significant impairment of 2-*O*-sulfation and induced compensatory increases in *N*- and 6-*O*-sulfation. Simultaneous block of *Hsepi* and HS 6-*O*-sulfotransferase (*Hs6st*) activity disrupted tracheoblast formation, a well established FGF-dependent process. This result suggests that the increase in 6-*O*-sulfation in *Hsepi* mutants is critical for the rescue of FGF signaling. We also found that the ectopic crossvein phenotype can be induced by expression of a mutant form of Hs2st with a strong substrate preference for GlcA-containing units, suggesting that this phenotype is associated with abnormal GlcA 2-*O*-sulfation. Finally, we show that Hsepi formed a complex with Hs2st and Hs6st in S2 cells, raising the possibility that this complex formation contributes to the close functional relationships between these enzymes.

HSPGs[2] play critical roles in a wide range of biological processes by regulating the action of growth factors, such as FGF, Wnt, TGF-β, and Hedgehog (1, 2). They are composed of a core protein and a long, negatively charged linear polysaccharide, heparan sulfate (HS). HS biosynthesis is a complex, multistep process. HS chains are polymerized by EXT proteins as unbranched, repeating disaccharides composed of *N*-acetylglucosamine (GlcNAc) and glucuronic acid (GlcA). During chain polymerization, *N*-deacetylase/*N*-sulfotransferase (NDST) removes the acetyl groups from some of the GlcNAc residues and replaces them with sulfate groups. After *N*-sulfation, glucuronyl C5-epimerase (Hsepi) converts GlcA to iduronic acid (IdoA) followed by *O*-sulfation events at specific ring positions. Because only a fraction of the potential targets are modified at each modification step, the resultant HS chain has considerable structural heterogeneity.

The biosynthesis of HS is controlled by a feedback mechanism known as "HS sulfation compensation," which was first recognized in the *Hs2st* mouse null mutant model (3). HS purified from *Hs2st*$^{-/-}$ mouse embryonic fibroblasts did not have 2-*O*-sulfate groups, but this loss was compensated by increased *N*- and 6-*O*-sulfation. Similarly, *Drosophila Hs2st* and *Hs6st* mutations induce compensatory increases in sulfation at 6-*O* and 2-*O* positions, respectively, restoring a wild-type net charge on HS in both genotypes (4). This compensation rescues FGF, Wingless, and BMP signaling pathways *in vivo*, thus ensuring the robustness of developmental systems (4, 5). However, the mechanism by which cells sense the lack of a specific sulfation event and induce a compensatory reaction is unknown.

The fact that a change in sulfation status at one ring position is responded to by a compensatory sulfation at other positions indicates that activities of multiple HS-modifying enzymes are tightly regulated. From this point of view, it is important to understand physical interactions between HS biosynthetic/modifying enzymes. It has been proposed that these enzymes form a physical complex called a "gagosome" to coordinate HS

* This work was supported, in whole or in part, by National Institutes of Health Grant R01 HD042769 (to H. N.).

[1] To whom correspondence should be addressed: Dept. of Genetics, Cell Biology, and Development, University of Minnesota, 321 Church St. S. E., Minneapolis, MN 55455. Tel.: 612-625-1727; Fax: 612-626-5652; E-mail: nakat003@umn.edu.

[2] The abbreviations used are: HSPG, heparan sulfate proteoglycan; HS, heparan sulfate; Hsepi, glucuronyl C5-epimerase; Hs2st, heparan sulfate 2-*O*-sulfotransferase; Hs6st, heparan sulfate 6-*O*-sulfotransferase; GlcNAc, *N*-acetylglucosamine; GlcA, glucuronic acid; IdoA, iduronic acid; pCV, posterior crossvein; NDST, *N*-deacetylase/*N*-sulfotransferase; BMP, *bone morphogenetic* protein; EXT, exostosin; GlcA2S, 2-*O*-sulfated GlcA; IdoA2S, 2-*O*-sulfated IdoA; *hh*, *hedgehog*; *btl*, *breathless*; *sfl*, *sulfateless*; *dlp*, *dally-like*; *sdc*, *syndecan*; UAS, upstream activation sequence; CS, chondroitin sulfate; ΔDi-0S, 2-acetamido-2-deoxy-3-*O*-(β-D-gluco-4-enepyranosyluronic acid)-D-galactose; ΔDi-4S, 2-acetamido-2-deoxy-3-*O*-(β-D-gluco-4-enepyranosyluronic acid)-4-*O*-sulfo-D-galactose.

synthesis (1, 6, 7). Previous studies have identified a physical association between Hsepi and Hs2st (6) and between NDST1 and EXT2 (8), supporting the gagosome model. What other components participate in the gagosome and how this complex regulates HS structures still remain elusive.

One of the least understood steps of HS biosynthesis is C5-epimerization of GlcA to IdoA catalyzed by Hsepi. Sulfation at the 2-*O* position of uronic acid occurs almost exclusively on IdoA residues and very rarely on GlcA (1, 9). For this reason, C5-epimerization of GlcA to IdoA is required for normal sulfation patterns and biological processes. It has been shown that genetic loss of *Hsepi* results in a wide array of developmental defects and lethality in several animal models, including mouse, zebrafish, and *Caenorhabditis elegans* (10–14). The disruption of the *Hsepi* gene largely phenocopied that of *Hs2st* in many of these models, consistent with the fact that 2-*O*-sulfation is dependent on C5-epimerization. $Hsepi^{-/-}$ mice die shortly after birth with renal agenesis, lung defects, and skeletal malformations (10). HS from the $Hsepi^{-/-}$ mutants was devoid of IdoA but showed increased *N*- and 6-*O*-sulfation. Kidney agenesis and skeletal abnormalities were also commonly observed in *Hs2st*-deficient mice, whereas the $Hs2st^{-/-}$ mice have normal lungs and survive a little longer than *Hsepi* mutants (15). In addition, *Hs2st*-deficient mice show mild reductions in the thickness of the cerebral cortex and the spinal cord in the brain (16). On the other hand, *Hsepi*-deficient mice did not show any defect in other organ systems, such as the brain and vasculature. Because normal development of these organs requires HS-dependent signaling pathways (17), the up-regulation of *N*- and 6-*O*-sulfation may rescue some signaling pathways. In fact, HS from the $Hsepi^{-/-}$ cells showed aberrant interactions with FGF2 and glia-derived neurotropic factor but interacted normally with FGF10 (18). However, the mechanism for the differential effects of *Hs2st* and *Hsepi* mutations on morphogenesis is not understood.

Despite the strong preference of Hs2st on the C2 position of IdoA over GlcA, it can add 2-*O*-sulfate groups to GlcA (19). The product of such reaction, GlcA2S, is found on only 1% of total disaccharide units in most naturally occurring HS. However, higher levels of GlcA2S were found in cerebral cortex (20). This suggested that GlcA2S may be biologically important, but its functional significance is unknown.

Here we demonstrate that *Drosophila Hsepi* mutants show only modest morphological defects, whereas they have a significantly shorter longevity than wild type. *Hsepi* mutation resulted in a significant reduction of 2-*O*-sulfation and induced increases in *N*- and 6-*O*-sulfation. The up-regulation of 6-*O*-sulfation was required for the rescue of tracheoblast formation. On the other hand, *Hsepi* appears to play a limited role in HS compensation in *Hs2st* mutants: biochemically, the lack of *Hsepi* reduced the level of compensatory increases in *N*- and 6-*O*-sulfation, but the difference was not detectable in phenotypic analyses. Based on similarities and differences of phenotypic and biochemical analyses of *Hs2st*, *Hsepi*, and *Hs2st Hsepi* double mutants as well as phenotypes induced by mutant forms of Hs2st, we discuss the roles of 2-*O*-sulfated GlcA in development. We propose two mechanisms, HS sulfation compensation and developmental roles of GlcA2S, as contributing factors for the mild phenotypes of *Hsepi* mutants. We also show that Hsepi formed a complex with both Hs2st and Hs6st in S2 cells, consistent with intimate functional relationship between these enzymes.

EXPERIMENTAL PROCEDURES

Fly Strains—The detailed information for fly strains used is described in FlyBase. All flies were maintained at 25 °C. Oregon-R was used as a wild-type strain. The following alleles were used as null or strong hypomorphic mutants for each gene: $Hs2st^{d267}$, $Hs6st^{d770}$ (4), $sulfateless^{03844}$ (sfl^{03844}) (21), $dally^{gem}$ (22), sdc^{48} (23), dlp^{1} (24), and $Sulf1^{P1}$ (25). Two deficiency strains, *Df(2R)ED1618* (42C4-43A1) and *Df(2R)cn88b* (42A1-E7), which eliminate the genomic region, including the *Hsepi* locus, were used for P-element imprecise excision and genetic assays to characterize excision alleles. *hedgehog* (*hh*)-*GAL4* and *breathless* (*btl*)-*GAL4* were used to induce expression of UAS transgenes and are described in FlyBase. Other transgenic lines used were *UAS-Hsepi RNAi*, *UAS-Hs6st RNAi*, and *UAS-GFP*.

To generate *Hsepi* mutations, a P-element, P{SUPor-P}-CG3194[KG02877] was excised by P-element transposase from P{ry+, Δ2–3} (99B). This excision was performed in the presence of one copy of deficiency chromosome (*Df(2R)ED1618*) to increase the efficiency of imprecise excision events. Imprecise excisions were screened by PCR using flanking primers to identify deletions, and the extent of each deletion was determined by sequencing PCR products that spanned the junction. To determine lethality of mutants, heterozygous mutants over a balancer were crossed to each other, and adult progenies with or without the balancer chromosome were counted. Only female adult wings were used to score adult wing phenotypes, such as chemosensory bristle formation, wing vein defect, and ectopic crossvein structures. Student's *t* test was used to calculate significance for phenotypic analyses, and log rank test was used for the longevity assay.

DNA Constructs and Transgenic Flies—Site-directed mutagenesis of *Drosophila Hs2st* was designed based on previous information on residues responsible for catalytic activity and substrate specificity of vertebrate Hs2st homologues (26, 27). *Hs2st[DEAD]* was constructed by introducing the mutations H139A and H141A. This construct is equivalent to H140A/H142A of vertebrate Hs2st, which showed complete loss of catalytic function (26). *Hs2st[IdoA]* and *Hs2st[GlcA]* were constructed by introducing the mutation Y93A (equivalent to Y94A of chick Hs2st) and R188A (equivalent to R189A of chick Hs2st), respectively. The chick Y94A mutant showed a substantial preference for IdoA-containing substrate over GlcA-containing substrate, whereas the chick R189A mutant showed activity exclusively with GlcA-containing substrate. *Hs2st[WT]* is a wild-type *Hs2st* construct. *Hs2st[WT]*, *Hs2st[DEAD]*, *Hs2st[IdoA]*, and *Hs2st[GlcA]* cDNAs were cloned into UAS.attB vector (a gift from K. Basler), and transgenic strains bearing these UAS constructs were generated by BestGene Inc. using ϕC31-mediated integration of respective plasmid DNA into Basler ZH line 68E (28). Construction of the Golgi-tethered form of Sulf1 (Sulf1[Golgi]-HA) was described previously (25).

Quantitative PCR—Ten 1-day-old female flies were homogenized in TRIzol reagent (Invitrogen) to isolate total RNA. The RNA samples were treated with RNase-free DNase I (Qiagen) and purified with the RNeasy Mini kit (Qiagen). cDNA was synthesized from 1 μg of purified RNA with the SuperScript III First-Strand Synthesis System for RT-PCR (Invitrogen). Quantitative PCR was performed in duplicate on each of three independent biological replicates in the Mx3000P qPCR System (Stratagene) using EvaGreen qPCR MasterMix (MidSci). *rp49* was used as a normalization control. The following primers were used: *rp49* forward, 5′-ACAGGCCCAAGATCGTGAAG-3′; *rp49* reverse, 5′-TGTTGTCGATACCCTTGGGC-3′; *sfl* forward, 5′-CACGCATTATGTCGATACGG-3′; *sfl* reverse, 5′-GTGTTTGCCACCAGAGTTGA-3′; *Hs2st* forward, 5′-TCGGAGTCACAGAGCAGATG-3′; *Hs2st* reverse, 5′-CCGCAGATGAGATTTGTTTG-3′; *Hs6st* forward, 5′-GCGCTCCAAAATCCGAACAA-3′; *Hs6st* reverse, 5′-CGTTTGGATAGGGCGCATAC-3′; *Sulf1* forward, 5′-CCTCAGGATCCATTGCTTGT-3′; *Sulf1* reverse, 5′-TCGGCTCCCCAGTATAGTCA-3′.

Immunohistochemistry and RNA in Situ Hybridization—Immunostaining was performed as described previously (29, 30). Adult ovaries and testes were dissected and fixed with 3.7% formaldehyde in PBS for 20 min at room temperature. Anti-FasIII was used to visualize ovarian somatic cells. To visualize actin filament in testes, Alexa Fluor 564-conjugated phalloidin was used. TOPRO-3 (Invitrogen) was used for nuclear counterstaining in the ovary and wing disc. Secondary antibodies were from the Alexa Fluor series (1:500; Molecular Probes).

In situ RNA hybridization was performed as described previously (25, 31). Imaginal discs were dissected from third instar larvae and fixed with 4% paraformaldehyde. Digoxigenin-labeled *Hsepi* RNA probes were synthesized using a DIG RNA Labeling kit (Roche Applied Science). Anti-digoxigenin antibody conjugated with alkaline phosphatase was used as a secondary antibody. The signal was developed by a standard protocol using 3,3′-diaminobenzidine as a substrate.

Co-immunoprecipitation and Immunoblot Analysis—cDNAs for *Hs2st*, *Hsepi*, and *Hs6st* were cloned into pAWH and pAWM vectors. Co-immunoprecipitation was performed as described previously (25, 32) using *Drosophila* S2 cells. Anti-Myc-agarose beads (Sigma) were used for co-immunoprecipitation. The eluted proteins were subjected to immunoblot analysis using mouse anti-Myc (9E10) (1:2,000; Sigma) and rat anti-HA antibodies (3F10) (1:2,000; Roche Applied Science).

Disaccharide Analysis—Glycosaminoglycan isolation and disaccharide composition analysis were carried out as described previously (4, 25, 33). Approximately 200 mg of adult flies was used to isolate glycosaminoglycans. The glycosaminoglycan sample was digested with a heparitinase mixture (Seikagaku), and the resulting disaccharide species were separated using reversed-phase ion pair chromatography. The effluent was monitored fluorometrically for postcolumn detection of HS disaccharides. Similarly, glycosaminoglycan sample was digested with chondroitinases, and compositions of unsaturated chondroitin sulfate (CS) disaccharides ΔDi-0S and ΔDi-4S were analyzed by reversed-phase ion pair chromatography.

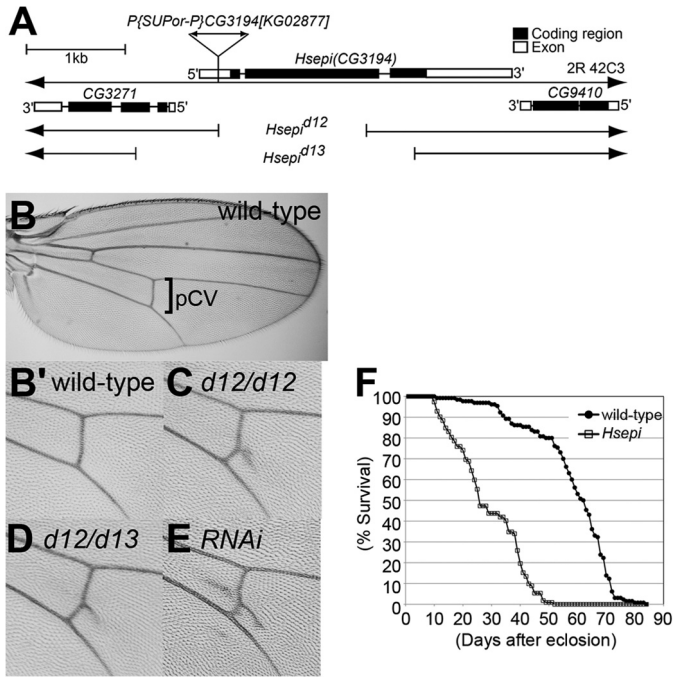

FIGURE 1. **Structure of *Drosophila Hsepi* gene.** *A*, schematic diagram of *Hsepi* genomic region. A P-element insertion, P{SUPor-P}CG3194[KG02877], was used for the imprecise excision to isolate excision alleles. *Filled boxes* and *open boxes* indicate the protein coding sequence and untranslated regions, respectively. $Hsepi^{d12}$ and $Hsepi^{d13}$ lack most of the protein coding sequence, including the residues critical for C5-epimerase enzymatic activity. $Hsepi^{d13}$ also removes the 5′-portion of an upstream gene, CG3271. *B–E*, ectopic vein formation of *Hsepi* mutants. Adult wings are shown for wild type (*B* and *B′*), $Hsepi^{d12}$ (*C*), $Hsepi^{d12}/Hsepi^{d13}$ (*D*), and *hh-Gal4/UAS-Hsepi RNAi* (*E*). High magnification views for the pCV region are presented (B′, *C*, *D*, and *E*). *F*, survival curve of wild-type (*closed circles*) and *Hsepi* mutant (*open boxes*) adult flies. A 57% decrease in mean survival was observed in *Hsepi* mutants ($n > 110$; log rank test, $p < 0.0001$).

RESULTS

Isolation of Drosophila Hsepi Mutants—The *Drosophila* genome has a single copy of *Hsepi* homologue as in the mammalian genome. To analyze the *in vivo* function of *Drosophila Hsepi*, we isolated mutations deleting the *Hsepi* locus by imprecise excision of a P-element inserted in the 5′-untranslated region of the *Hsepi* gene. The isolated $Hsepi^{d12}$ and $Hsepi^{d13}$ alleles remove virtually the entire *Hsepi* coding sequence (Fig. 1*A*). Sequencing analysis of genomic DNA isolated from these mutants showed that both alleles lack most of the protein coding sequence, including the region containing multiple histidine and tyrosine residues crucial for C5-epimerase enzymatic activity (34), suggesting that they are molecularly null. The $Hsepi^{d13}$ allele additionally removes the 5′-portion of an upstream gene, CG3271. The homozygous mutants for $Hsepi^{d12}$ and $Hsepi^{d13}$ are viable and fertile with modest levels of lethality at larval and pupal stages (Table 1). We confirmed the amorphic nature of $Hsepi^{d12}$ by genetic experiments using a deficiency line, *Df(2R)cn88b*, which lacks the cytological region 42A1-E7, including the entire *Hsepi* locus. Lethality of $Hsepi^{d12}$ homozygotes (18.3%) was equivalent to that of their deficiency transheterozygotes ($Hsepi^{d12}/Df(2R)cn88b$; 19.3%), indicating that it is a null allele. We used $Hsepi^{d12}$ allele for the following experiments.

TABLE 1
Lethality of mutants for HS-modifying enzymes
Lethality was determined using the following alleles: $Hsepi^{d12}$, $Hs2st^{d267}$, $Hs6st^{d770}$, and $Sulf1^{P1}$. For each genotype, more than 100 progenies were counted.

Genotype	Lethality
	%
Hsepi	18.3
Hsepi/Df(2R)cn88b	19.3
Hs2st	27.6
Hs2st Hsepi	37.5
Hs6st	21.0
Hsepi; Hs6st	100.0
Sulf1	8.0
Hsepi; Sulf1	62.0
Hsepi; dally	100.0

Adult survivors show only modest morphological phenotypes, such as extra vein materials at the posterior crossvein (pCV) region of the wing (Fig. 1*C*). The penetrance of this phenotype was 25% in males and 90% in females ($n > 100$). This phenotype was also observed in $Hsepi^{d12}/Hsepi^{d13}$ transallelic mutants (Fig. 1*D*; penetrance >90%, $n > 100$) as well as *Hsepi* RNAi animals (*hh-Gal4/UAS-Hsepi RNAi*; Fig. 1*E*; penetrance >90%, $n > 100$), confirming the specificity of this phenotype. Despite relatively normal development and fertility of the adult survivors of *Hsepi* mutants, the longevity of mutant adults is remarkably shorter than wild type (Fig. 1*F*). The median of adult longevity of *Hsepi* mutants was 27 days, whereas it was 63 days in wild type. Thus, mutation of *Hsepi* has a relatively modest effect on morphogenesis and development but is indispensable for normal lifespan. Although the mechanism by which *Hsepi* ensures normal lifespan remains to be elucidated, given that HSPGs are essential regulators of female germ line stem cells (35), it is possible that *Hsepi* affects longevity through its functions in adult stem cell niches.

Expression Patterns of Hsepi mRNA—We next examined expression patterns of *Hsepi* mRNA during development by RNA *in situ* hybridization. We found that *Hsepi* is expressed ubiquitously throughout larval tissues, including the wing disc (Fig. 2*A*), eye-antennal disc (Fig. 2*B*), and larval CNS (Fig. 2*D*). This is consistent with the idea that C5-epimerization is a critical step in HS biosynthesis and required in all cells that produce HSPGs.

In situ hybridization also revealed non-uniform expression patterns of *Hsepi* mRNA in several tissues. For example, high levels of *Hsepi* mRNA were detected in the nurse cells in the adult ovary (Fig. 2*C*). We recently found that Syndecan is expressed on the surface of nurse cells (data not shown). We have shown previously that glypicans play critical roles in somatic cells in the ovary, affecting germ line development (35, 36). The findings of *Hsepi*/*Syndecan* expression in the nurse cells suggest a possible cell-autonomous role of HSPGs in germ line cells. It is also likely that a portion of *Hsepi* mRNA may be transported to the oocyte to be stored as maternal mRNA for embryogenesis.

The *Hsepi* transcript was detected at much higher levels in the morphogenetic furrow of the eye disc (Fig. 2*B*) and at the lamina furrow of the optic lobe (Fig. 2, *D* and *E*) than in other cells in these organs. It is worth noting that these cells express high levels of *Hs2st* (Fig. 2*F* and data not shown) and *dally*, which encodes a core protein of the glypican family of HSPGs (37). It is therefore possible that these cells have a higher level of activity of the HS biosynthetic machinery.

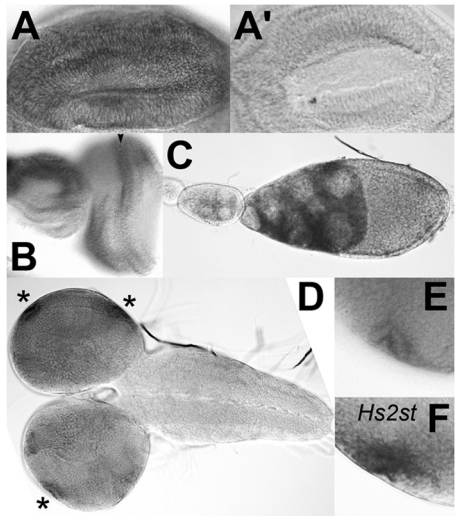

FIGURE 2. ***In situ* hybridization of *Hsepi* mRNA.** *A–E*, *in situ* hybridization revealed ubiquitous but non-uniform expression of *Hsepi* mRNA in various tissues, including the wing disc (*A* and *A′*), eye-antennal disc (*B*), adult ovary (*C*), and larval CNS (*D* and *E*). High levels of *Hsepi* expression were detected in the morphogenetic furrow in the eye disc (*C*, *arrowhead*) and in the lamina furrow in the optic lobe of the CNS (*D*, *asterisks*). *E* shows a high magnification view of the lamina furrow. *F* shows the same region of the CNS as *E* that was hybridized with an *Hs2st* antisense probe. *A′* shows a control wing disc hybridized with an *Hsepi* sense probe.

Disaccharide Structures of Hsepi Mutant HS—To study the effect of *Hsepi* mutation on HS sulfation patterns, disaccharide structures of HS isolated from *Hsepi* mutants were analyzed. HS was isolated from *Hsepi* and *Hs2st* mutant adults and completely digested into disaccharides by heparitinase, and the differentially modified disaccharide species were separated by high performance liquid chromatography. Although this assay does not distinguish GlcA- and IdoA-containing disaccharide units, it provides valuable information regarding HS structures from the mutants.

As reported previously (4), HS from *Hs2st*-null mutants showed a complete loss of 2S-containing disaccharide units with a remarkable increase of 6-*O*-sulfated disaccharides (Table 2 and Fig. 3*A*). We have shown previously that this compensatory increase in 6-*O*-sulfation restores FGF signaling during tracheal system formation (4). The compensation mechanism also rescues Wingless and BMP signaling (5).

We found that overall disaccharide patterns of *Hsepi* mutant HS were similar to those of *Hs2st*. *Hsepi* mutant HS showed a substantial reduction of 2-*O*-sulfate groups, reflecting the strong preference of Hs2st for IdoA as a substrate, and a parallel increase of *N*- and 6-*O*-sulfate groups (Table 2 and Fig. 3*A*). Thus, *Hsepi* mutation also induces compensatory up-regulation of 6-*O*-sulfation as observed in *Hs2st*. This suggests that the mild morphological phenotypes of *Hsepi* mutants are due to the compensatory increase in 6-*O*-sulfation as shown in *Hs2st*. Although overall patterns were similar, there were a couple of notable differences between the two mutants. First, a residual peak was detectable for the ΔUA2S-GlcNS unit. Because *Hsepi*-null animals produce no IdoA-containing units, this peak should represent GlcA2S. In fact, GlcA2S was found to be

TABLE 2

Disaccharide analyses of HS from Hsepi, Hs2st, and Hs2st Hsepi double mutant animals

The disaccharide composition of HS is shown for each respective genotype. The values are given as mol % of total disaccharides and represent mean ± S.D. from three independent experiments. NAc, ΔUA-GlcNAc; NS, ΔUA-GlcNS; NAc6S, ΔUA-GlcNAc6S; NS6S, ΔUA-GlcNS6S; 2SNS, ΔUA2S-GlcNS; and 2SNS6S, ΔUA2S-GlcNS6S; ND, not detectable. A graphical depiction of these results is shown in Fig. 3.

	HS (unsaturated disaccharide)					
	NAc	NS	NAc6S	NS6S	2SNS	2SNS6S
			%			
Wild type	37.5 ± 1.2	25.4 ± 0.7	2.0 ± 0.2	17.6 ± 0.7	14.2 ± 0.4	3.3 ± 0.4
Hsepi	30.4 ± 0.9	35.4 ± 0.4	1.2 ± 0.1	32.4 ± 0.8	0.5 ± 0.1	ND
Hs2st	36.2 ± 1.2	25.1 ± 0.3	2.0 ± 0.1	36.7 ± 1.0	ND	ND
Hs2st Hsepi	29.2 ± 0.9	41.4 ± 0.5	0.8 ± 0.1	28.5 ± 0.6	ND	ND

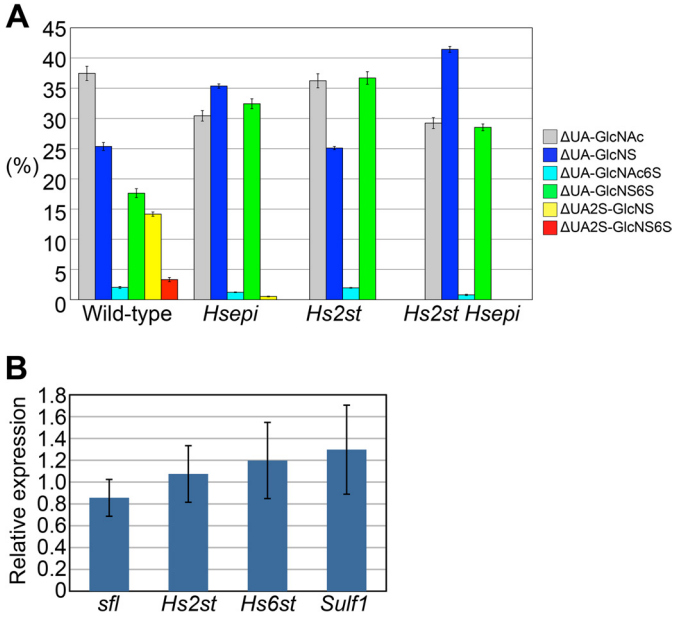

FIGURE 3. **HS disaccharide profiling of *Hsepi* mutants.** *A*, graphical depiction of disaccharide composition of HS from each respective genotype. Bar graphs show percentages of the following disaccharides: ΔUA-GlcNAc (*gray*), ΔUA-GlcNS (*blue*), ΔUA-GlcNAc6S (*light blue*), ΔUA-GlcNS6S (*green*), ΔUA2S-GlcNS (*yellow*), and ΔUA2S-GlcNS6S (*red*). The values were obtained from three independent experiments, and each *bar* represents the mean ± S.D. *B*, quantitative PCR analysis of the mRNA levels of the indicated genes in *Hsepi* mutants relative to wild-type animals. Data are presented as the mean fold change with S.D. ($n = 6$). Expression levels of *sfl*, *Hs2st*, *Hs6st*, and *Sulf1* genes are not significantly altered in *Hsepi* mutants ($p > 0.1$). *Error bars* represent S.D.

increased in HS from *Hsepi*$^{-/-}$ mice (18). Second, the increase of 6-*O*-sulfation was less prominent in *Hsepi* compared with *Hs2st*. Instead, a significant increase of NS was observed in *Hsepi* but not in *Hs2st* mutants. These features are consistent with the results obtained in *Hsepi*$^{-/-}$ mice (10, 18).

Does C5-epimerization play a role in HS sulfation compensation? To determine whether *Hsepi* affects the compensatory increase in the level of 6-*O*-sulfation in *Hs2st* mutants, we examined the disaccharide profile of HS from *Hs2st Hsepi* double mutants. If C5-epimerization is important for HS compensation, one can expect that *Hs2st Hsepi* mutant HS does not have as high levels of 6-*O*-sulfation as that from *Hs2st* single mutants. We found that this was the case. In the double mutants, the level of NS6S units was significantly lower than in *Hs2st*, indicating that *Hs2st* mutation cannot efficiently increase 6-*O*-sulfation in the absence of *Hsepi* activity. These results indicated that, at the biochemical level, *Hsepi* contributes to at least a portion of the compensatory elevation of 6-*O*-sulfation in *Hs2st* mutants. With the reduction of 6-*O*-sulfation in the double mutants, reflected by the decreased level of NS6S units, there was a concurrent increase of NS units when compared with *Hs2st* single mutants. As a result, *Hsepi* mutation led to an increase of the *N*-sulfation/*O*-sulfation ratio.

TABLE 3

Disaccharide analyses of chondroitin sulfate from Hsepi, Hs2st, and Hs2st Hsepi double mutant animals

The composition of unsaturated CS disaccharides ΔDi-0S and ΔDi-4S is shown for each respective genotype.

	CS (unsaturated disaccharide)	
	ΔDi-0S	ΔDi-4S
	%	
Wild type	87.7	12.3
Hsepi	87.5	12.5
Hs2st	88.0	12.0
Hs2st Hsepi	90.2	9.8

We asked whether *Hs2st*, *Hsepi*, or *Hs2st Hsepi* mutations affect disaccharide composition of CS. Digestion of glycosaminoglycans with chondroitinases yields two disaccharide species, ΔDi-0S and ΔDi-4S (33). The ratio of these CS disaccharide units was not significantly altered in these mutant flies (Table 3). This result confirmed the HS-specific effects of these mutations.

Because *N*- and 6-*O*-sulfate groups were increased in *Hsepi* mutants, we asked whether or not this change was accomplished by up-regulated expression of *sfl*, which encodes the only *Drosophila* NDST, and/or *Hs6st*. RT-quantitative PCR analysis revealed that expression levels of *sfl*, *Hs2st*, *Hs6st*, and *Sulf1* genes were not significantly altered in *Hsepi* mutants (Fig. 3*B*). This result suggests that the compensatory sulfation changes in *Hsepi* mutants occur mainly through a mechanism that is independent of transcriptional control of HS-modifying enzymes.

Germ Line Development in Hs2st and in Hsepi Mutants—Because *Hsepi* mutation significantly reduced 2-*O*-sulfation, we compared phenotypes between *Hs2st* and *Hsepi* mutants. The most obvious difference between these mutants is their fertility. We have previously reported that *Hs2st* mutant flies develop all the way to adult stage, but both males and females of *Hs2st* mutant adults are completely sterile (4, 36). However, *Hsepi* mutant flies are viable and fertile. To understand the cellular basis for the fertility and sterility of these mutants, we analyzed the morphology of mutant ovaries. In particular, we focused on stalk formation, which is known to require HSPG activity. The stalk cells are a special type of follicle cells that separate developing egg chambers. The stalk cell differentiation is regulated by Jak/Stat signaling, and we recently demonstrated that this control is dependent on two glypican genes, *dally* and *dally-like* (*dlp*) (36). Dally and Dlp serve as co-receptors for Unpaired, a

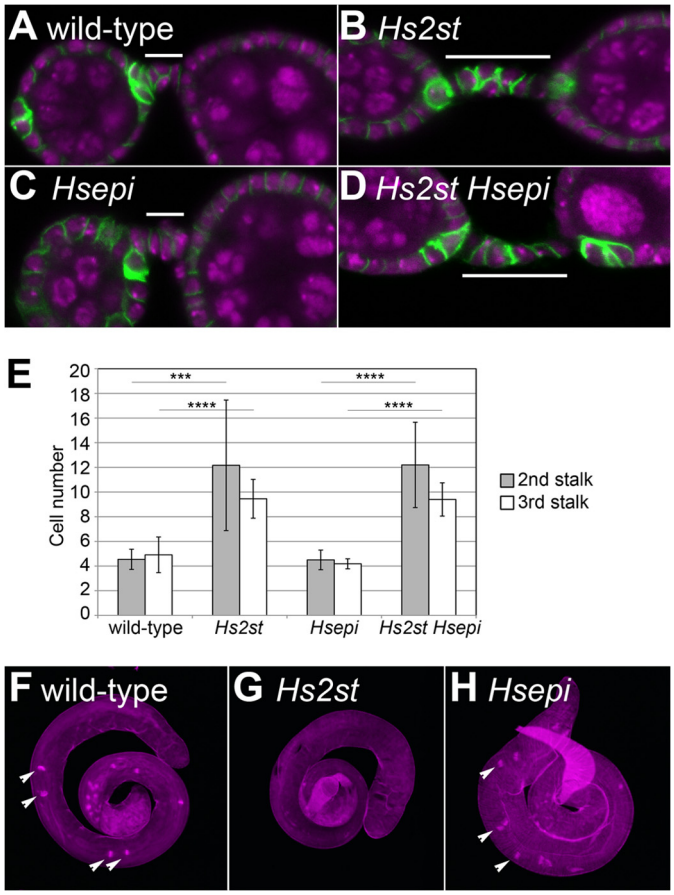

FIGURE 4. **Germ line development in *Hs2st* and *Hsepi* mutants.** *A–D*, the ovaries are shown for wild-type (*A*), *Hs2st* (*B*), *Hsepi* (*C*), and *Hs2st Hsepi* (*D*) by staining with anti-FasIII antibody (*green*) and TOPRO-3 (*magenta*). The second stalk is marked with *white bars*. *E*, quantification of cell number in the second (*gray*) and third (*white*) stalks of the indicated genotypes is shown. ***, $p < 0.001$; ****, $p < 0.0001$; $n > 25$ for each genotype. *Error bars* represent S.D. *F–H*, testes from wild-type (*F*), *Hs2st* (*G*), and *Hsepi* (*H*) flies are shown. The penetrance of the *Hs2st* testis phenotype is 100% ($n = 20$). Staining with phalloidin (*magenta*) highlights the investment cones (*arrowheads*).

ligand of the *Drosophila* Jak/Stat pathway, and stalk cells are lost in mutant clones for *sfl* or *dally*/*dlp*. On the other hand, *Hs2st* mutant ovarioles showed an increased number of stalk cells (Fig. 4, *B* and *E*, and Ref. 36). Although the molecular mechanism of this defect is not fully understood, it is possible that Upd ligand distribution is altered in *Hs2st* mutants. In contrast, *Hsepi* mutants did not show this defect: the stalk cell number of *Hsepi* was almost the same as that of wild type (Fig. 4, *C* and *E*). We examined the stalk cell number of *Hs2st Hsepi* double mutants to investigate their genetic relationship. We found that the stalk cell phenotype in *Hs2st Hsepi* double mutants was closely similar to *Hs2st* single mutant flies with no obvious additional effect of *Hsepi* mutation to the *Hs2st* mutant phenotype (Fig. 4, *D* and *E*).

We also analyzed the male gonads of these mutants. *Hs2st* mutant testes are smaller than those of wild type (Fig. 4*G*). Phalloidin staining revealed the loss of the investment cones, which are a characteristic structure for elongated spermatids (38), suggesting that maturation of male germ cells failed in *Hs2st* mutant testes (Fig. 2, *H–J*). In contrast, overall morphology of *Hsepi* mutant testes was normal (Fig. 4*H*).

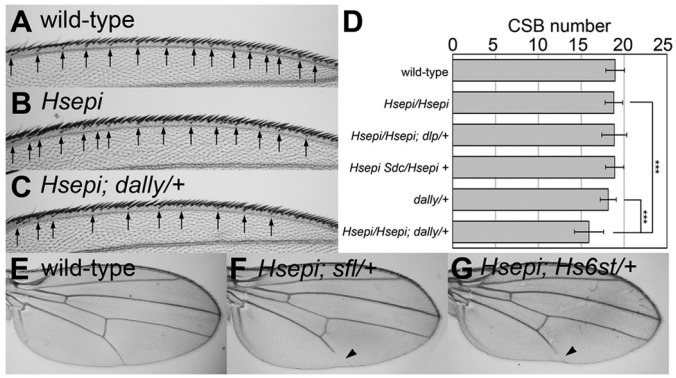

FIGURE 5. **Genetic interactions between *Hsepi* and HSPG core protein/HS-modifying enzyme genes.** *A–C*, dorsal view of anterior wing margin of female wild-type (*A*), *Hsepi* (*B*), and *Hsepi; dally/+* (*C*) adult wings. The *arrows* indicate positions of chemosensory bristles. *D*, bar graphs showing the number of chemosensory bristles (*CSB*) in female wings of the indicated genotypes. ***, $p < 0.001$. *Error bars* represent S.D. *E–G*, female adult wings are shown for wild-type (*E*), *Hsepi; sfl/+* (*F*), and *Hsepi; Hs6st/+* (*G*). *Arrowheads* point to truncated wing vein V.

These analyses as well as normal fertility of *Hsepi* adult flies indicated that, unlike *Hs2st*, *Hsepi* appears to be dispensable for germ line development. The phenotypic difference between *Hs2st* and *Hsepi* mutant flies suggests that 2-*O*-sulfation but not C5-epimerization of HS chains plays critical roles in this process. Given that there should be no IdoA in the *Hsepi* mutant flies due to the loss of C5-epimerization activity, the existence of 2-*O*-sulfated GlcA may be sufficient for germ line development.

Genetic Interactions between Hsepi and HSPG Core Protein Genes during Wing Margin Formation—To further analyze the role of *Hsepi* in development, we examined the genetic interactions between *Hsepi* and HSPG core protein genes. Previous studies have established that HSPGs regulate multiple patterning events during wing/notum development, including the formation of sensory bristles at the wing margin (29), wing veins (37), and tracheoblast in the wing disc (4). In this study, we used these phenotypes as readouts for our genetic interaction assays.

It has been shown previously that the number of chemosensory bristles is reduced in *dally* mutant flies (29, 39, 40). This reflects the reduced Wingless signaling at the wing margin of the mutants. Bristle number was not affected in *Hsepi* homozygous mutants (Fig. 5*B*). In *dally* heterozygous mutants, the average number of these bristles was slightly lower than wild type, but the difference was not statistically significant (Fig. 5*D*). In contrast, heterozygosity of *dally* in the *Hsepi* homozygous mutant background (*Hsepi*/*Hsepi; dally*/+) resulted in a decreased number of chemosensory bristles (Fig. 5, *C* and *D*). On the other hand, we did not detect such synergistic effect by deleting one copy of other HS core protein genes, *dlp* and *syndecan* (*sdc*), in this particular developmental context (Fig. 5*D*). These results suggest that Hsepi modifies HS chains on Dally during wing margin formation.

Remarkably, we found that *Hsepi* and *dally* double mutants were completely lethal (Table 1). This strong genetic interaction suggests that Dally is an important substrate for Hsepi. In addition, this synthetic lethal effect also indicates that Hsepi acts on the other HSPG core proteins too in another developmental process. If *Hsepi* only modified HS chains on Dally, then

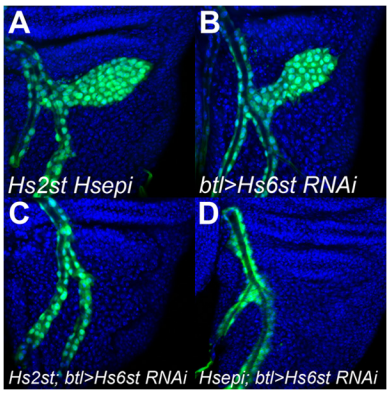

FIGURE 6. **6-*O*-Sulfation is required for the rescue of tracheoblast formation in *Hsepi* mutants.** Tracheoblast formation is shown in *Hs2st Hsepi; btl-Gal4 UAS-GFP/+* (*A*), *btl-Gal4 UAS-GFP/UAS-Hs6st RNAi* (*B*), *Hs2st; btl-Gal4 UAS-GFP/UAS-Hs6st RNAi* (*C*), *Hsepi; btl-Gal4 UAS-GFP/UAS-Hs6st RNAi* (*D*). Tracheal cells are visualized by *UAS-GFP* expression driven by *btl-Gal4* (*green*). *Blue* shows counterstaining by TOPRO-3.

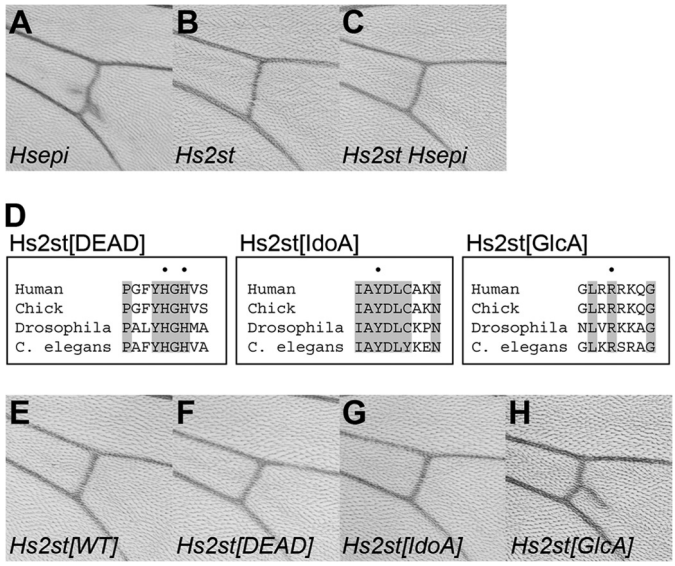

FIGURE 7. **Ectopic vein phenotype is associated with elevated 2-*O*-sulfated GlcA.** *A–C*, the pCV region of adult wings is shown for *Hs2st* (*A*), *Hsepi* (*B*), and *Hs2st Hsepi* (*C*) mutants. *D*, alignment of Hs2st amino acid sequences from different organisms (human, chick, *Drosophila*, and *C. elegans*). Sequences around vertebrate Hs2st His-140/His-142 (Hs2st[DEAD]), Tyr-94 (Hs2st[IdoA]), and Arg-189 (Hs2st[GlcA]) are shown. Positions of these residues are *dotted*, and residues conserved among all four species are *highlighted*. To generate each *Drosophila* mutant construct, the *dotted* residues were substituted to Ala. *E–H*, the pCV region of adult wings is shown for *hh-Gal4/UAS-Hs2st[WT]* (*E*), *hh-Gal4/UAS-Hs2st[DEAD]* (*F*), *hh-Gal4/UAS-Hs2st[IdoA]* (*G*), and *hh-Gal4/UAS-Hs2st[GlcA]* (*H*).

dally would be genetically epistatic to *Hsepi* (phenotypes of *Hsepi; dally* would be the same as *dally* single mutants). Thus, the phenotypic differences between *dally* (semilethal) and *Hsepi; dally* (lethal) reflect the function of other HSPG molecules.

Genetic Interactions between Hsepi and HS-modifying Enzymes during Wing Vein Formation—We next examined the genetic interaction between *Hsepi* and other HS-modifying enzymes. No abnormality was observed in longitudinal wing vein structures of *Hsepi* homozygous mutant flies (data not shown). Similarly, heterozygous mutants of *sfl* (*sfl*/+) have wild-type wings. In contrast, heterozygosity of *sfl* in the *Hsepi* homozygous mutant background (*Hsepi*/*Hsepi; sfl*/+) resulted in a truncation of longitudinal vein L5 (Fig. 5*F*; the penetrance was 85.3% in female, $n = 34$). Similarly, *Hsepi*/*Hsepi; Hs6st*/+ also showed a reduction of the wing vein L5, whereas the penetrance was lower than that in *Hsepi*/*Hsepi; sfl*/+ (Fig. 5*G*; the penetrance was 51.9% in female, $n = 52$). These synergistic enhancements of *Hsepi* phenotypes by these mutations reflect intimate functional relationships of these HS modification enzymes during wing vein formation.

An Increase in 6-O-Sulfation Is Critical for the Rescue of Tracheoblast Formation in Hsepi Mutants—We have shown previously that the compensatory increase of 6-*O*-sulfation in *Hs2st* mutants is critical for the rescue of the mutants and that *Hs2st; Hs6st* double mutants fail to restore FGF, Wingless, and BMP signaling (4, 5). Our disaccharide analysis data revealed a substantial increase 6-*O*-sulfation in *Hsepi* mutants as observed in *Hs2st* mutants (Fig. 3). Therefore, we hypothesized that this increased 6-*O*-sulfation plays a role in the restoration of developmental pathways and the survival of *Hsepi* mutants. In fact, *Hsepi; Hs6st* double mutants are completely lethal (Table 1). To further test this idea, we analyzed the effect of *Hs6st* RNAi on FGF signaling during tracheoblast formation, a well known FGF-dependent process, in an *Hsepi* mutant background. No defect was observed in tracheoblasts in *Hsepi* mutant wing discs (data not shown) as reported in *Hs2st* mutants (4). Similarly, tracheoblasts of *Hs2st Hsepi* double mutants were indistinguishable from wild type (Fig. 6*A*). In addition, we did not detect any defect when an *Hs6st* RNAi construct was expressed in tracheoblasts by a *breathless-Gal4* driver at 25 °C (*btl>Hs6st RNAi*) (Fig. 6*B*; $n = 24$). We have shown that the knockdown of *Hs6st* in this condition partially but significantly reduces *Hs6st* mRNA levels (5). In contrast, as we have reported previously (4), *Hs6st* knockdown in the same condition under *Hs2st* mutant background (*Hs2st; btl>Hs6st RNAi*) severely interfered with tracheoblast formation (Fig. 6*C*; penetrance, 50.0%; $n = 24$). We observed the same effect in *Hsepi* or in *Hs2st Hsepi* backgrounds: tracheoblast formation was strongly blocked in *Hsepi; btl>Hs6st RNAi* (Fig. 6*D*; penetrance, 50.0%; $n = 24$) and in *Hs2st Hsepi; btl>Hs6st RNAi* (data not shown). These results suggest that tracheoblast formation in *Hsepi* mutants is rescued by increased 6-*O*-sulfation as observed in *Hs2st* mutants.

Ectopic Vein Phenotype Is Associated with Elevated 2-O-Sulfated GlcA—As stated above, *Hsepi* mutants showed ectopic vein materials at the pCV region (Figs. 1, *C–E*, and 7*A*). Interestingly, this phenotype was not observed in *Hs2st*-null mutant wings (Fig. 7*B*). In addition, *Hs2st Hsepi* double mutants did not exhibit this phenotype, indicating that the ectopic pCV phenotype of *Hsepi* mutants was suppressed by *Hs2st* mutation (Fig. 7*C*). Given that HS from *Hsepi* mutants but not *Hs2st* or *Hs2st Hsepi* double mutants includes GlcA2S, these results raised the possibility that the ectopic pCV phenotype may be associated with abnormal GlcA 2-*O*-sulfation.

To test this hypothesis, we generated mutant forms of *Drosophila Hs2st* based on previous structure-based mutational studies of vertebrate Hs2sts that identified residues responsible for the catalytic activity and substrate specificity of these enzymes (Refs. 26 and 27 and Fig. 7*D*). For example, histidine residues at 140 and 142 are important for catalysis, and the double mutant H140A/H142A resulted in complete loss of activity

(26). Several amino acid residues that had an impact on substrate specificity were also identified: Y94A and R189A mutants showed a substantial preference for IdoA-containing and GlcA-containing substrates, respectively. All these residues are completely conserved in *Drosophila* Hs2st (Fig. 7*D*). In fact, these residues are perfectly conserved in all Hs2st homologues from various species thus far available in GenBank™, supporting the evolutionary conservation of the function of these specific residues. We generated three mutant constructs, *Hs2st[DEAD]*, *Hs2st[IdoA]*, and *Hs2st[GlcA]*, that bear mutations equivalent to vertebrate H140A/H142A, Y94A, and R189A, respectively. Transgenic strains bearing UAS constructs for each mutant cDNA as well as wild-type *Hs2st* were generated by site-specific integration at the genomic location 68E (28). Overexpression of wild-type *Hs2st* in the posterior compartment of the developing wing by the *hh-Gal4* driver did not show any obvious defect in the adult wing (Fig. 7*E*), consistent with a previous report (41). Similarly, no pCV phenotype was observed in the wings overexpressing *Hs2st[DEAD]* or *Hs2st[IdoA]* (Fig. 7, *F* and *G*; $n > 20$ for each genotype). In contrast, overexpression of *Hs2st[GlcA]* by *hh-Gal4* produced ectopic vein materials at the pCV region, mimicking the phenotype observed in *Hsepi* mutant flies (Fig. 7*H*; penetrance, 94.7%; $n = 19$). Because these UAS transgenes have been integrated into the same genomic location, the phenotypic difference reflects the activity of each construct rather than differential expression levels due to positional effects. Taken together, these results support the idea that the ectopic pCV phenotype is associated with increased levels of GlcA2S.

Physical Interaction of HS Modification Enzymes—It has been shown that Hs2st and Hsepi form a complex in mammalian cultured cells (6). We first tested whether this physical interaction is conserved in *Drosophila* enzymes by co-immunoprecipitation experiments. *Drosophila* S2 cells were co-transfected with Myc-tagged Hsepi and HA-tagged Hs2st expression constructs. Upon immunoprecipitation of Hsepi-Myc from a protein extract of the transfected cells, Hs2st-HA was detected in the immunoprecipitates by immunoblotting (Fig. 8*A*). This result indicated that, as in the case of mammalian homologues, *Drosophila* Hsepi and Hs2st physically interact with one another in S2 cells.

The sulfation compensation system requires a close functional relationship between *Hs2st* and *Hs6st*: 6-*O*-sulfation was increased in response to the loss of Hs2st or Hsepi. Therefore, we tested the possibility that Hs6st also physically interacts with Hsepi or Hs2st. Similar co-immunoprecipitation experiments revealed that Hs6st-HA was co-immunoprecipitated with both Hs2st-Myc and Hsepi-Myc (Fig. 8, *B* and *C*). This finding suggests that these three HS modification enzymes can form a molecular complex in S2 cells. Neither wild type (data not shown) nor the Golgi-tethered form of Sulf1, an extracellular HS 6-*O*-endosulfatase, showed an interaction with Hsepi (Fig. 8*D*), supporting that the observed binding among Hsepi-Hs2st-Hs6st is specific.

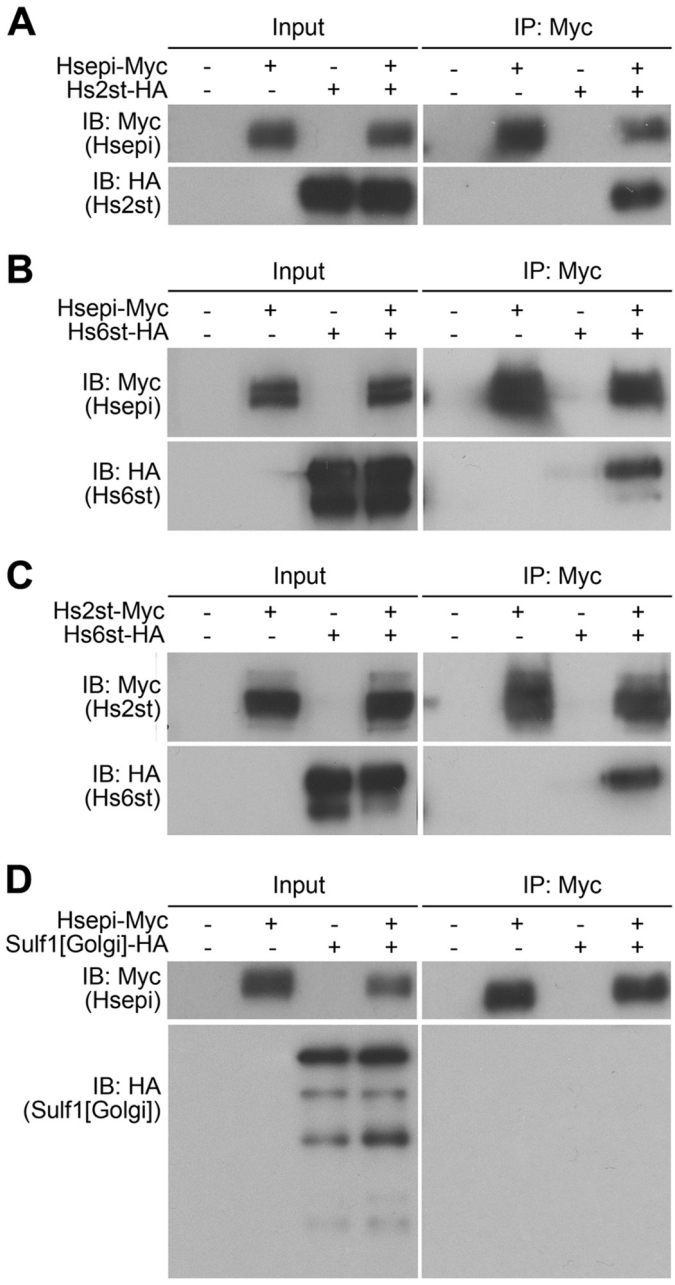

FIGURE 8. **Physical interaction of Hs2st, Hs6st, and Hsepi in S2 cells.** Co-immunoprecipitation results are shown for Hsepi-Myc and Hs2st-HA (*A*), Hsepi-Myc and Hs6st-HA (*B*), Hs2st-Myc and Hs6st-HA (*C*), and Hsepi-Myc and the Golgi-tethered form of Sulf1 (Sulf1[Golgi]-HA) (*D*). Myc-tagged proteins were recovered from cell lysate by anti-Myc-agarose beads and eluted with urea. Precipitates were analyzed by immunoblotting using anti-HA and anti-Myc antibodies. *IP*, immunoprecipitation; *IB*, immunoblotting.

DISCUSSION

Previous studies have shown that *Hsepi* function is critical for normal animal development (10–14). C5-Epimerization plays a crucial role for signal transduction by providing a substrate for 2-*O*-sulfation (42). Furthermore, it has been suggested that FGF2 signaling is dependent on the synthesis of IdoA rather than on 2-*O*-sulfation *per se* (18). We found that overall *Drosophila Hsepi*-null mutants are significantly healthier than *Hs2st* mutants. For example, *Hs2st* but not *Hsepi* mutants showed morphological defects in both female and male gonads, leading to sterility. This was an unexpected finding since C5-epimerization is an upstream event of 2-*O*-sulfation, which is known to be heavily dependent on the epimerization reac-

tion. In addition, *Hsepi*$^{-/-}$ mice showed defects equivalent to or more severe than those of *Hs2st*$^{-/-}$ mice, leading to lethality at earlier stages (10, 18). One mechanism that appears to contribute to the mild phenotypes of *Hsepi* mutants is HS sulfation compensation. We showed that 6-*O*-sulfation is dramatically elevated in these mutants. Thus, compensatory up-regulation of 6-*O*-sulfate groups may be responsible for rescue of HS-dependent pathways in *Hsepi* mutant flies as observed in *Hs2st* mutant animals (4, 5). Consistent with this idea, *Hsepi; Hs6st* mutants are completely lethal (Table 1). Tracheal cell-specific knockdown of *Hs6st* in an *Hsepi* mutant background inhibited tracheoblast formation (Fig. 6); thus, the increased 6-*O*-sulfation indeed rescued this FGF-dependent process. Another possible mechanism for the mild phenotypes observed in *Hsepi* mutants is that GlcA2S-containing units play a role and contribute to tissue patterning. This issue is discussed later.

Despite the clear importance of increased 6-*O*-sulfation in rescuing *Hs2st* and *Hsepi* mutant phenotypes, it is not understood how this compensation occurs. In *Hs2st* mutants, 6-*O*-sulfation is up-regulated in compensation, rescuing morphogenesis and HS-dependent molecular pathways, including FGF, Wnt, and BMP signaling (4, 5). Our HS disaccharide analyses revealed that the increase of 6-*O*-sulfation in *Hs2st* mutants in the absence of *Hsepi* was not as remarkable as that in its presence. Thus, at the biochemical level, *Hsepi* is required for efficient HS sulfation compensation in *Hs2st* mutants. However, its role appeared to be relatively minor at the physiological level. If *Hsepi* activity is critical for *Hs2st* mutants to increase 6-*O*-sulfation, then one can expect *Hs2st Hsepi* double mutants to show more severe phenotypes compared with *Hs2st* mutants due to incomplete HS sulfation compensation. However, we detected no obvious difference between *Hs2st* and *Hs2st Hsepi* mutant phenotypes. Therefore, the reduction of the compensatory increase of 6-*O*-sulfation in *Hs2st Hsepi* detected in the disaccharide analysis may not cause any additional failure in rescuing signaling pathways. We observed strong genetic interactions between *Hsepi* and *Hs6st*. *Hsepi; Hs6st* double mutants were completely lethal, and *Hs6st* RNAi in an *Hsepi* mutant background inhibited tracheoblast formation, suggesting that *Hsepi* is required for HS sulfation compensation in *Hs6st* mutants. This is not surprising given that 2-*O*-sulfation was dramatically reduced in *Hsepi* mutants. Thus, the effect of *Hsepi* on the compensation mechanism in *Hs6st* may be indirect: *Hsepi* is important for 2-*O*-sulfation, which is critical for the rescue of *Hs6st* mutants.

Although the mechanism for HS sulfation compensation is unknown, it is achieved through close functional interactions between HS-modifying enzymes. From this respect, our finding that Hs6st physically interacted with Hs2st and Hsepi is intriguing. The gagosome was defined as a physical complex of HS biosynthetic/modifying enzymes committed to the assembly of HS (1). It was also proposed that the composition of the gagosome would affect HS fine structure. Physical interactions were shown for Hs2st and Hsepi (6) and for NDST and EXT2 (8). The existence of a complex of Hs2st and Hsepi with Hs6st raises an interesting possibility that the formation of a gagosome complex is important for proper sulfation compensation. Given that loss of one type of sulfation results in an increase of sulfation at different positions during sulfation compensation, gagosome complexes with different component compositions may have different kinetics. For example, a complex lacking Hs6st may have an enhanced Hs2st activity. Further study is needed to elucidate the *in vivo* mechanism of this remarkable feedback system.

Hsepi mutants showed ectopic vein formation at the pCV region. Because remarkably this phenotype was suppressed by *Hs2st* mutation, we hypothesized that this phenotype is associated with GlcA2S. Consistent with this model, we found that overexpression of an Hs2st mutant protein that preferentially adds a 2-*O*-sulfate group on GlcA phenocopies *Hsepi* mutant wings. Thus, abnormal crossvein formation is the first example of a specific developmental event that is associated with elevated GlcA2S levels. Furthermore, our results suggest that GlcA2S-containing units play a role in a specific developmental pathway, supporting the idea that it may rescue developmental processes in *Hsepi* mutants that are more severely affected in *Hs2st* mutants, such as germ line development. It is not known how GlcA2S can compensate for the lack of IdoA2S. Similarly, it is unknown how HS from *Hs2st* or *Hs6st* mutants can still mediate HS-dependent signaling pathways to some extent. One explanation for both phenomena would be that such HS chains are flexible enough to twist and bend to place sulfate groups at appropriate three-dimensional positions and form hydrogen bonds to specific residues of ligand proteins. It has been established that pCV formation is controlled by BMP signaling. In the pupal wing, a BMP ligand, Decapentaplegic, is expressed only in the longitudinal veins and directionally transported to the pCV primordial region (43–46). This directional transport is facilitated by the extracellular BMP-binding proteins Short gastrulation (Sog) and Crossveinless (Cv) (46). The formation of ectopic vein materials at the pCV suggests the failure of proper movement of BMP ligands toward the pCV position. It has been suggested that HSPGs are involved in pCV formation (39, 47). The phenotypes of *Hsepi* mutants and *hh>Hs2st[GlcA]* animals suggests that precise regulation of HS structures, particularly the levels of GlcA2S, is responsible for the directional transport of BMPs. However, the molecular mechanism for this control remains to be elucidated.

Acknowledgments—We are grateful to K. Basler, the Developmental Studies Hybridoma Bank, and the Bloomington Stock Center for reagents. We thank Dan Levings for helpful discussions and critical reading of the manuscript.

REFERENCES

1. Esko, J. D., and Selleck, S. B. (2002) Order out of chaos: assembly of ligand binding sites in heparan sulfate. *Annu. Rev. Biochem.* **71,** 435–471
2. Kirkpatrick, C. A., and Selleck, S. B. (2007) Heparan sulfate proteoglycans at a glance. *J. Cell Sci.* **120,** 1829–1832
3. Merry, C. L., and Gallagher, J. T. (2002) New insights into heparan sulphate biosynthesis from the study of mutant mice. *Biochem. Soc. Symp.* 47–57
4. Kamimura, K., Koyama, T., Habuchi, H., Ueda, R., Masu, M., Kimata, K., and Nakato, H. (2006) Specific and flexible roles of heparan sulfate modifications in *Drosophila* FGF signaling. *J. Cell Biol.* **174,** 773–778
5. Dejima, K., Kleinschmit, A., Takemura, M., Choi, P. Y., Kinoshita-Toyoda, A., Toyoda, H., and Nakato, H. (2013) The role of *Drosophila* heparan sulfate 6-*O*-endosulfatase in sulfation compensation. *J. Biol. Chem.* **288,**

6574–6582
6. Pinhal, M. A., Smith, B., Olson, S., Aikawa, J., Kimata, K., and Esko, J. D. (2001) Enzyme interactions in heparan sulfate biosynthesis: uronosyl 5-epimerase and 2-O-sulfotransferase interact *in vivo*. *Proc. Natl. Acad. Sci. U.S.A.* **98,** 12984–12989
7. Ledin, J., Ringvall, M., Thuveson, M., Eriksson, I., Wilén, M., Kusche-Gullberg, M., Forsberg, E., and Kjellén, L. (2006) Enzymatically active *N*-deacetylase/*N*-sulfotransferase-2 is present in liver but does not contribute to heparan sulfate *N*-sulfation. *J. Biol. Chem.* **281,** 35727–35734
8. Presto, J., Thuveson, M., Carlsson, P., Busse, M., Wilén, M., Eriksson, I., Kusche-Gullberg, M., and Kjellén, L. (2008) Heparan sulfate biosynthesis enzymes EXT1 and EXT2 affect NDST1 expression and heparan sulfate sulfation. *Proc. Natl. Acad. Sci. U.S.A.* **105,** 4751–4756
9. Smeds, E., Feta, A., and Kusche-Gullberg, M. (2010) Target selection of heparan sulfate hexuronic acid 2-O-sulfotransferase. *Glycobiology* **20,** 1274–1282
10. Li, J. P., Gong, F., Hagner-McWhirter, A., Forsberg, E., Abrink, M., Kisilevsky, R., Zhang, X., and Lindahl, U. (2003) Targeted disruption of a murine glucuronyl C_5-epimerase gene results in heparan sulfate lacking L-iduronic acid and in neonatal lethality. *J. Biol. Chem.* **278,** 28363–28366
11. Bülow, H. E., and Hobert, O. (2004) Differential sulfations and epimerization define heparan sulfate specificity in nervous system development. *Neuron* **41,** 723–736
12. Ghiselli, G., and Farber, S. A. (2005) D-Glucuronyl C5-epimerase acts in dorso-ventral axis formation in zebrafish. *BMC Dev. Biol.* **5,** 19
13. Feyerabend, T. B., Li, J. P., Lindahl, U., and Rodewald, H. R. (2006) Heparan sulfate C5-epimerase is essential for heparin biosynthesis in mast cells. *Nat. Chem. Biol.* **2,** 195–196
14. Townley, R. A., and Bülow, H. E. (2011) Genetic analysis of the heparan modification network in *Caenorhabditis elegans*. *J. Biol. Chem.* **286,** 16824–16831
15. Bullock, S. L., Fletcher, J. M., Beddington, R. S., and Wilson, V. A. (1998) Renal agenesis in mice homozygous for a gene trap mutation in the gene encoding heparan sulfate 2-sulfotransferase. *Genes Dev.* **12,** 1894–1906
16. Merry, C. L., and Wilson, V. A. (2002) Role of heparan sulfate-2-O-sulfotransferase in the mouse. *Biochim. Biophys. Acta* **1573,** 319–327
17. Grobe, K., Ledin, J., Ringvall, M., Holmborn, K., Forsberg, E., Esko, J. D., and Kjellén, L. (2002) Heparan sulfate and development: differential roles of the N-acetylglucosamine N-deacetylase/N-sulfotransferase isozymes. *Biochim. Biophys. Acta* **1573,** 209–215
18. Jia, J., Maccarana, M., Zhang, X., Bespalov, M., Lindahl, U., and Li, J. P. (2009) Lack of L-iduronic acid in heparan sulfate affects interaction with growth factors and cell signaling. *J. Biol. Chem.* **284,** 15942–15950
19. Rong, J., Habuchi, H., Kimata, K., Lindahl, U., and Kusche-Gullberg, M. (2001) Substrate specificity of the heparan sulfate hexuronic acid 2-O-sulfotransferase. *Biochemistry* **40,** 5548–5555
20. Lindahl, B., Eriksson, L., and Lindahl, U. (1995) Structure of heparan sulphate from human brain, with special regard to Alzheimer's disease. *Biochem. J.* **306,** 177–184
21. Lin, X., and Perrimon, N. (1999) Dally cooperates with *Drosophila* Frizzled 2 to transduce Wingless signalling. *Nature* **400,** 281–284
22. Tsuda, M., Kamimura, K., Nakato, H., Archer, M., Staatz, W., Fox, B., Humphrey, M., Olson, S., Futch, T., Kaluza, V., Siegfried, E., Stam, L., and Selleck, S. B. (1999) The cell-surface proteoglycan Dally regulates Wingless signalling in *Drosophila*. *Nature* **400,** 276–280
23. Johnson, K. G., Ghose, A., Epstein, E., Lincecum, J., O'Connor, M. B., and Van Vactor, D. (2004) Axonal heparan sulfate proteoglycans regulate the distribution and efficiency of the repellent slit during midline axon guidance. *Curr. Biol.* **14,** 499–504
24. Kirkpatrick, C. A., Dimitroff, B. D., Rawson, J. M., and Selleck, S. B. (2004) Spatial regulation of Wingless morphogen distribution and signaling by Dally-like protein. *Dev. Cell* **7,** 513–523
25. Kleinschmit, A., Koyama, T., Dejima, K., Hayashi, Y., Kamimura, K., and Nakato, H. (2010) *Drosophila* heparan sulfate 6-O endosulfatase regulates Wingless morphogen gradient formation. *Dev. Biol.* **345,** 204–214
26. Xu, D., Song, D., Pedersen, L. C., and Liu, J. (2007) Mutational study of heparan sulfate 2-*O*-sulfotransferase and chondroitin sulfate 2-*O*-sulfotransferase. *J. Biol. Chem.* **282,** 8356–8367
27. Bethea, H. N., Xu, D., Liu, J., and Pedersen, L. C. (2008) Redirecting the substrate specificity of heparan sulfate 2-O-sulfotransferase by structurally guided mutagenesis. *Proc. Natl. Acad. Sci. U.S.A.* **105,** 18724–18729
28. Bischof, J., Maeda, R. K., Hediger, M., Karch, F., and Basler, K. (2007) An optimized transgenesis system for *Drosophila* using germ-line-specific ϕC31 integrases. *Proc. Natl. Acad. Sci. U.S.A.* **104,** 3312–3317
29. Fujise, M., Izumi, S., Selleck, S. B., and Nakato, H. (2001) Regulation of dally, an integral membrane proteoglycan, and its function during adult sensory organ formation of *Drosophila*. *Dev. Biol.* **235,** 433–448
30. Fujise, M., Takeo, S., Kamimura, K., Matsuo, T., Aigaki, T., Izumi, S., and Nakato, H. (2003) Dally regulates Dpp morphogen gradient formation in the *Drosophila* wing. *Development* **130,** 1515–1522
31. Kamimura, K., Fujise, M., Villa, F., Izumi, S., Habuchi, H., Kimata, K., and Nakato, H. (2001) *Drosophila* heparan sulfate 6-*O*-sulfotransferase (dHS6ST) gene. Structure, expression, and function in the formation of the tracheal system. *J. Biol. Chem.* **276,** 17014–17021
32. Akiyama, T., Kamimura, K., Firkus, C., Takeo, S., Shimmi, O., and Nakato, H. (2008) Dally regulates Dpp morphogen gradient formation by stabilizing Dpp on the cell surface. *Dev. Biol.* **313,** 408–419
33. Toyoda, H., Kinoshita-Toyoda, A., and Selleck, S. B. (2000) Structural analysis of glycosaminoglycans in *Drosophila* and *Caenorhabditis elegans* and demonstration that *tout-velu*, a *Drosophila* gene related to EXT tumor suppressors, affects heparan sulfate *in vivo*. *J. Biol. Chem.* **275,** 2269–2275
34. Li, K., Bethea, H. N., and Liu, J. (2010) Using engineered 2-*O*-sulfotransferase to determine the activity of heparan sulfate C_5-epimerase and its mutants. *J. Biol. Chem.* **285,** 11106–11113
35. Hayashi, Y., Kobayashi, S., and Nakato, H. (2009) *Drosophila* glypicans regulate the germline stem cell niche. *J. Cell Biol.* **187,** 473–480
36. Hayashi, Y., Sexton, T. R., Dejima, K., Perry, D. W., Takemura, M., Kobayashi, S., Nakato, H., and Harrison, D. A. (2012) Glypicans regulate JAK/STAT signaling and distribution of the Unpaired morphogen. *Development* **139,** 4162–4171
37. Nakato, H., Futch, T. A., and Selleck, S. B. (1995) The division abnormally delayed (dally) gene: a putative integral membrane proteoglycan required for cell division patterning during postembryonic development of the nervous system in *Drosophila*. *Development* **121,** 3687–3702
38. White-Cooper, H. (2004) Spermatogenesis: analysis of meiosis and morphogenesis. *Methods Mol. Biol.* **247,** 45–75
39. Takeo, S., Akiyama, T., Firkus, C., Aigaki, T., and Nakato, H. (2005) Expression of a secreted form of Dally, a *Drosophila* glypican, induces overgrowth phenotype by affecting action range of Hedgehog. *Dev. Biol.* **284,** 204–218
40. Kirkpatrick, C. A., Knox, S. M., Staatz, W. D., Fox, B., Lercher, D. M., and Selleck, S. B. (2006) The function of a *Drosophila* glypican does not depend entirely on heparan sulfate modification. *Dev. Biol.* **300,** 570–582
41. Kamimura, K., Maeda, N., and Nakato, H. (2011) *In vivo* manipulation of heparan sulfate structure and its effect on *Drosophila* development. *Glycobiology* **21,** 607–618
42. Casu, B., and Lindahl, U. (2001) Structure and biological interactions of heparin and heparan sulfate. *Adv. Carbohydr. Chem. Biochem.* **57,** 159–206
43. Ralston, A., and Blair, S. S. (2005) Long-range Dpp signaling is regulated to restrict BMP signaling to a crossvein competent zone. *Dev. Biol.* **280,** 187–200
44. Serpe, M., Ralston, A., Blair, S. S., and O'Connor, M. B. (2005) Matching catalytic activity to developmental function: tolloid-related processes Sog in order to help specify the posterior crossvein in the *Drosophila* wing. *Development* **132,** 2645–2656
45. Shimmi, O., Ralston, A., Blair, S. S., and O'Connor, M. B. (2005) The crossveinless gene encodes a new member of the Twisted gastrulation family of BMP-binding proteins which, with Short gastrulation, promotes BMP signaling in the crossveins of the *Drosophila* wing. *Dev. Biol.* **282,** 70–83
46. Matsuda, S., and Shimmi, O. (2012) Directional transport and active retention of Dpp/BMP create wing vein patterns in *Drosophila*. *Dev. Biol.* **366,** 153–162
47. Chen, J., Honeyager, S. M., Schleede, J., Avanesov, A., Laughon, A., and Blair, S. S. (2012) Crossveinless d is a vitellogenin-like lipoprotein that binds BMPs and HSPGs, and is required for normal BMP signaling in the *Drosophila* wing. *Development* **139,** 2170–2176